

Supporting Information

Arsenoplatin-1 Is a Dual Pharmacophore Anticancer Agent

Đenana Miodragović,^{†,§} Antonello Merlino,^{*,‡} Elden P. Swindell,[†] Abraham Bogachkov,[†] Richard W. Ahn,[†] Sara Abuhadba,[§] Giarita Ferraro,[#] Tiziano Marzo,[−] Andrew P. Mazar,^{||} Luigi Messori^{*,#} and Thomas V. O'Halloran^{*,†}

[†]Chemistry of Life Processes Institute, Northwestern University, 2145 Sheridan Road, Evanston, Illinois 60208, United States

[‡]Department of Chemical Sciences, University of Naples Federico II, Complesso Universitario di Monte Sant'Angelo, Via Cintia, I-80126 Napoli, Italy

[§]Northeastern Illinois University, 5500 North St Louis Avenue, Chicago, Illinois 60625, United States

^{||}Pharmacology, Feinberg School of Medicine, Northwestern University, 2145 Sheridan Road, Evanston, Illinois 60208, United States

[−]Department of Pharmacy, University of Pisa, Via Bonanno Pisano 6, 56126, Pisa, Italy

[#]Department of Chemistry 'Ugo Schiff', Università degli Studi Firenze, via della Lastruccia, 3-13, 50019 Sesto Fiorentino, Italy

Corresponding Authors:

antonello.merlino@unina.it

luigi.messori@unifi.it

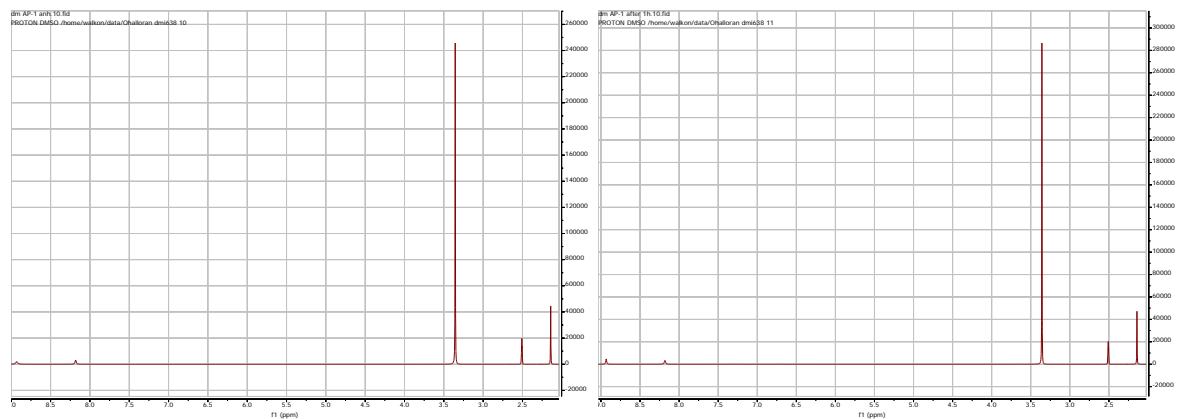
t-ohalloran@northwestern.edu

Table of Contents	Page
Solubility and Stability of Arsenoplatin-1	S3
Figure S1: ^1H NMR spectra of AP-1 in DMSO- d_6	S4
Figure S2: UV/Vis spectra of AP-1 in PBS	S5
Figure S3: ^{195}Pt NMR spectrum of AP-1 in $\text{CH}_3\text{OH}-d_4$	S6
NCI-60 human tumor cell lines screen	S7
Figure S4: One dose mean graph for Arsenoplatin-1 (AP-1)	S8
Figure S5: One dose mean graph for Cisplatin	S9
Figure S6: One dose mean graph for Arsenic Trioxide	S10
Figure S7: AP-1 vs As_2O_3 response in the NCI-60 screen	S11
Figure S8: AP-1 vs Cisplatin response in the NCI-60 screen	S11
ESI MS spectra	S12
Figure S9: Isotope pattern theoretical simulation and ESI -MS spectrum of AP-1-RNase A adduct	S12-S13
Crystallographic data	S14
Figure S10. Arsenoplatin-1-Lysozyme adduct – ribbon representation of structure (5NJ1)	S15
Catalytic Activity Assay	S16
Figure S11: Hydrolysis of yeast RNA by RNase A and by RNase A-AP-1 adduct	S16
DNA isolation using the DNazol Reagent	S17
Dose Response Studies	S18
Synergy Calculations	S18
Table S1: ^{195}Pt NMR chemical shifts	S19
Table S2: IC_{50} data from synergy studies	S19
Table S3: Data collection statistics	S20
Table S4: Refinement statistics	S21
Table S5: Lipinski rule of five and $\text{Log}P$ values	S22
References	S23-S24

Solubility and Stability of Arsenoplatin-1

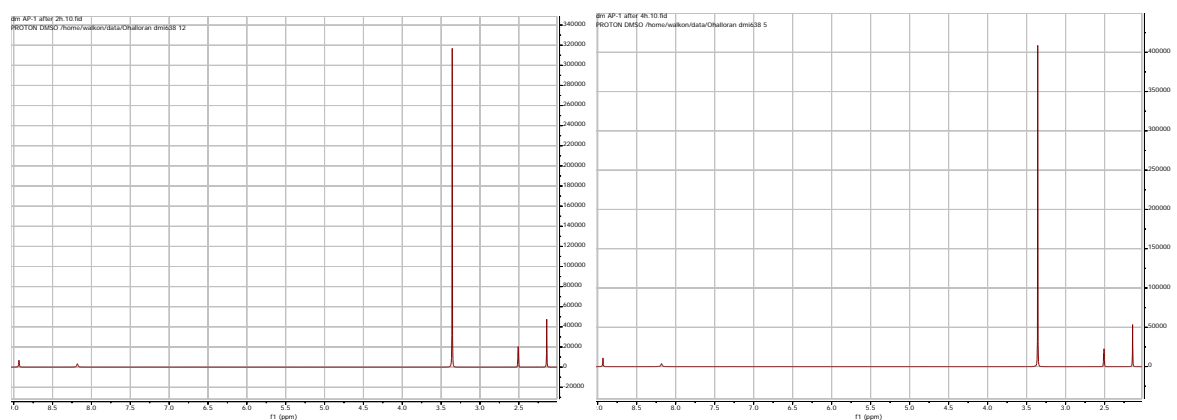
Arsenoplatin-1 is highly soluble in DMSO and in CH₃OH. DMSO solutions of candidate drug compounds are employed in many biological assays, including in the NCI-60 screen used here. We evaluated the stability of AP-1 in DMSO-d₆ in the 48h time period (Figure S1). The ¹H NMR chemical shifts for AP-1 dissolved in DMSO do not change and no new peaks were observed over a 48h period at 25°C. These observations support the argument that the Pt-Cl bond in AP-1 does not undergo solvolysis in DMSO. A comparison of the ¹⁹⁵Pt NMR spectra for AP-1 in DMSO-d₆¹ and methanol-d₄ (Figure S3) reveals a chemical shift difference of 36 ppm which is much smaller than the difference expected if DMSO replaced chloride in a Pt(II) compound: ¹⁹⁵Pt chemical shifts undergo an upfield shift of between 850-1,000 ppm when DMSO is substituted for chloride ion¹² (Table S1). Based on these results, we conclude that AP-1 is stable, with the Pt-Cl bond remaining intact, in DMSO solutions at 25°C over a 48h period.

Arsenoplatin 1 is slightly soluble in aqueous buffers, and it is stable in PBS (pH=7.4) solution for more than 48h (Figure S2).



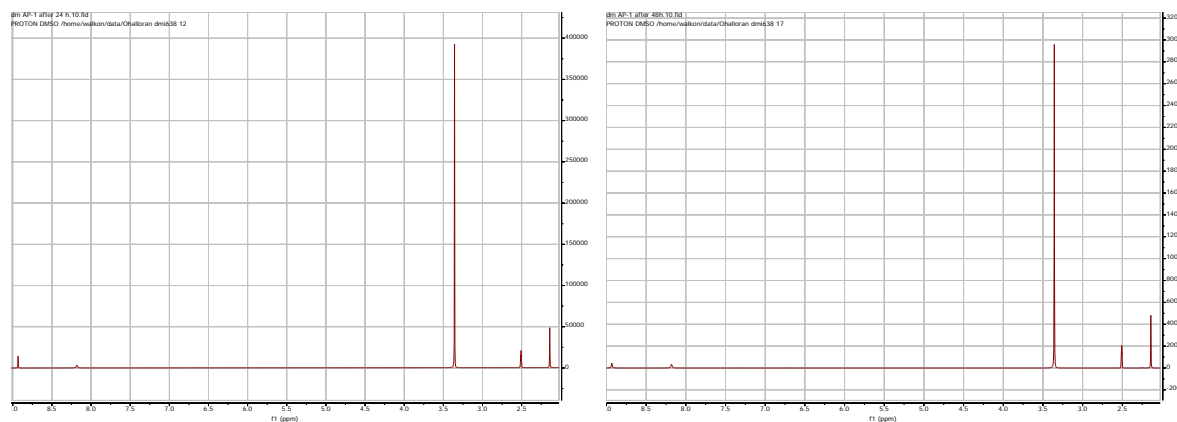
A

B



C

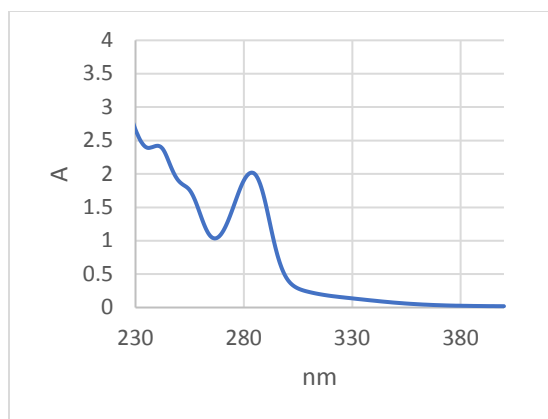
D



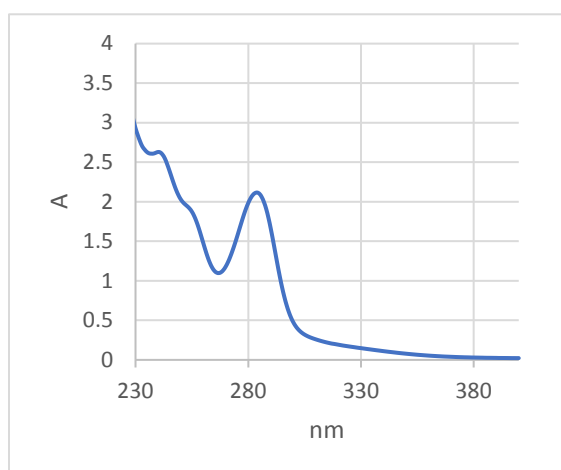
E

F

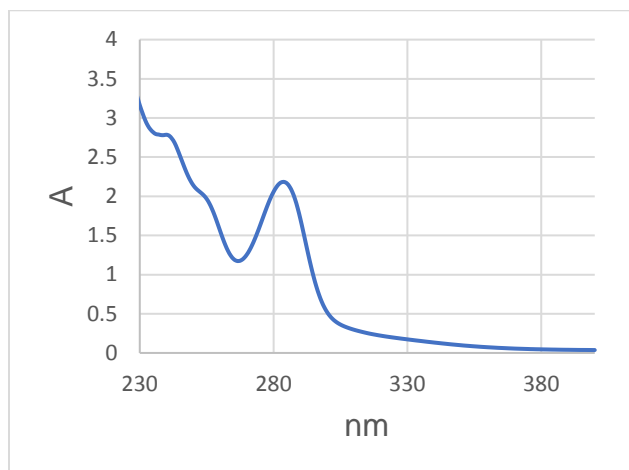
Figure S1. ¹H NMR spectrum of AP-1 in [D₆]DMSO solution, acquired at 500 MHz at 25 °C; ¹H referenced to residual [D₅H]DMSO at 2.50 ppm: **A**) after 15 min, **B**) after 1h, **C**) after 2h, **D**) after 4h, **E**) after 24h and **F**) after 48h at 25°C. (Chemical shifts in all spectra: 8.93 ppm (s, 2H-OH); 8.18 ppm (s, 2H-NH); 2.14 ppm (s, 6H-CH₃).



A)



B)



C)

Figure S2. AP-1 is slightly soluble in buffered solutions: in phosphate buffered saline (PBS) at pH = 7.4 solubility is 5 mg/mL and in saline alone (0.9 % NaCl) solubility is 4.5 mg/mL. Electronic absorption spectra indicate buffered solutions of AP-1 are stable over a 48h period: UV/Vis spectra of AP-1 dissolved in PBS (pH = 7.4) at 22°C (conc. 1 mg AP-1/5 ml PBS): A) after dissolving, B) after 24h, and C) after 48h. The maxima are at the same wavelengths in all spectra: $\lambda_1 = 284$ nm (sh. at 255 nm) and λ_2 at 240 nm. The slightly higher absorbance in the second and the third spectrum is due to slow evaporation of the solvent.

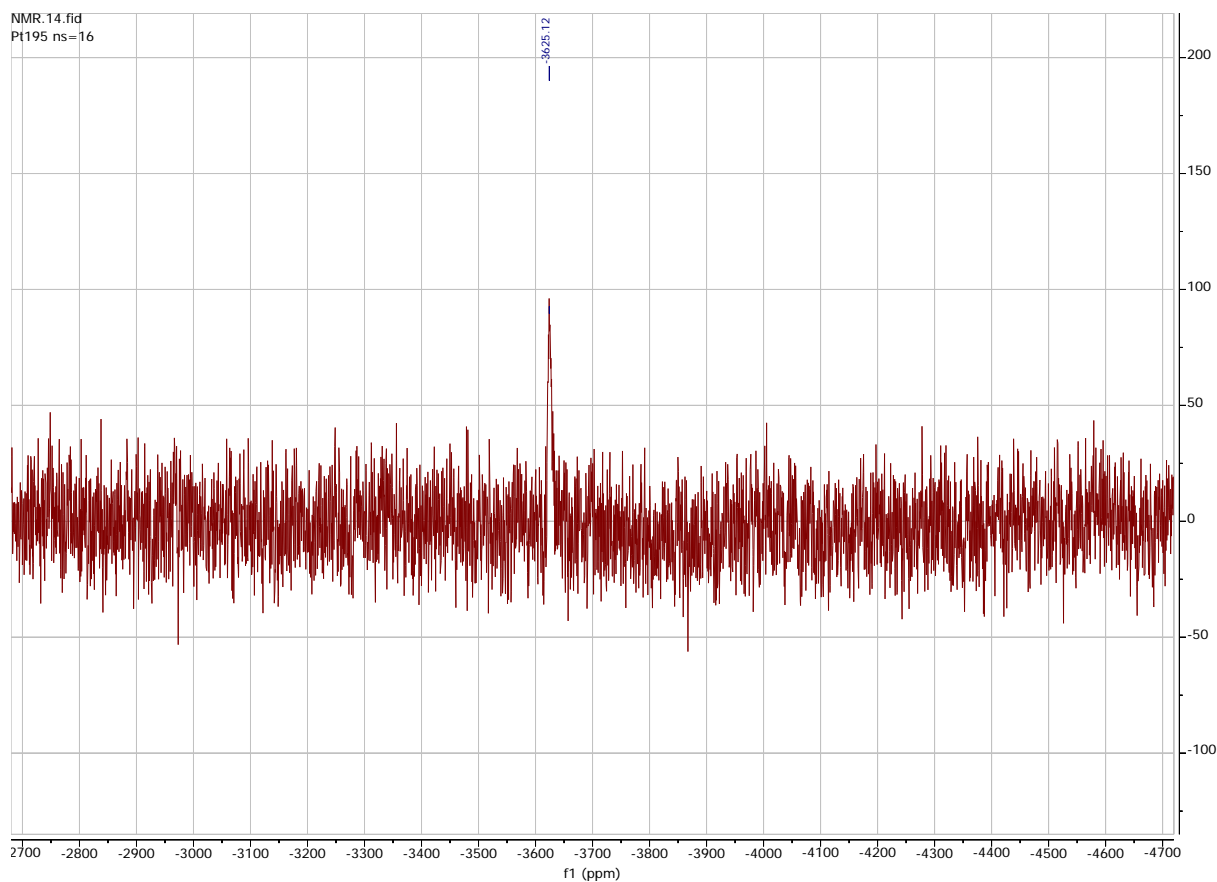


Figure S3. ^{195}Pt NMR spectrum of AP-1 acquired at 129 MHz (600 MHz ^1H) in $\text{CH}_3\text{OH-d}_4$ solution at 25 °C (^{195}Pt NMR chemical shifts were referenced indirectly to TMS in ^1H NMR spectrum such that $\text{K}_2^{195}\text{PtCl}_6$ in D_2O would resonate at 0.0 ppm). $\delta = -3625$ (s, 1Pt).

The ^{195}Pt (129 MHz) NMR spectrum was acquired on a 600 MHz (^1H) Bruker Avance III spectrometer equipped with BBFO smart probe.

NCI-60 Human Tumor Cell Lines Screen

NCI-60 screen is performed at the Developmental Therapeutics Core at Northwestern University.

Cell lines:

Leukemia: CCRF-CEM, HL-60(TB), K-562, MOLT-4, RPMI-8226 and SR

Non-Small Cell Lung: A549/ATCC, EKVX, HOP-62, HOP-92, NCI-H226, NCI-H23, NCI-H322M, NCI-H460 and NCI-H522

Colon: COLO 205, HCC-2998, HCT-116, HCT-15, HT29, KM12 and SW-620

CNS: SF-268, SF-295, SF-539, SNB-19, SNB-75 and U251

Melanoma: LOX IMVI, MALME-3M, M14, MDA-MB-435, SK-MEL-2, SK-MEL-28, SK-MEL-5, UACC-257 and UACC-62

Ovarian: IGR-OV1, OVCAR-3, OVCAR-4, OVCAR-5, OVCAR-8, NCI/ADR-RES and SK-OV-3

Renal: 786-0, A498, ACHN, CAKI-1, RXF 393, SN12C, TK-10 and UO-31

Prostate: PC-3 and DU-145

Breast: MCF7, MDA-MB-231/ATCC, MDA-MB-468, HS 578T, BT-549 and T-47D

Media: The cells were cultured in RPMI 1640 media supplemented with 10% Fetal Bovine Serum (FBS), 2mM glutamine and with 5% CO₂ and 37⁰C. For the experiment, 5% of FBS and 50 ug/mL of gentamycin were used.

Compounds tested: 10 µM solutions of AP-1, Cisplatin, and Arsenic Trioxide. The drugs and AP-1 were dissolved in DMSO and then diluted with media so that the final concentration of the drugs and AP-1 was 10 µM, and the final concentration of DMSO in the wells with the drugs and AP-1, as well as in the control wells, was 0.1%.

Study: Cells were plated in 96 well plates in triplicate at the densities based on NCI recommendation. Time zero cells (Tz) will be fixed the following day with 50% (for adherent cells) or 80% (for suspension cells) ice cold trichloroacetic acid (TCA) and washed 5x with water. At 48 hours post addition of treatments, all remaining plates were fixed in 80% ice cold trichloroacetic acid (TCA) and washed 5x with water. After drying, one hundred microliters of 0.4% Sulphorhodamine B (SRB) in 1% acetic acid was added to each plate including the Tzero plate and incubated for 10 minutes at room temperature. After 5 additional washes with 1% acetic acid, plates were allowed to dry. One hundred microliters of Trizma base was added to each well and plates were read at 515 nm. Results obtained were submitted to the NCI and the COMPARE algorithm was used to generate the one dose mean graphs for AP-1, Cisplatin, and Arsenic Trioxide.

Developmental Therapeutics Program Mean Graph
Selected Data Vectors

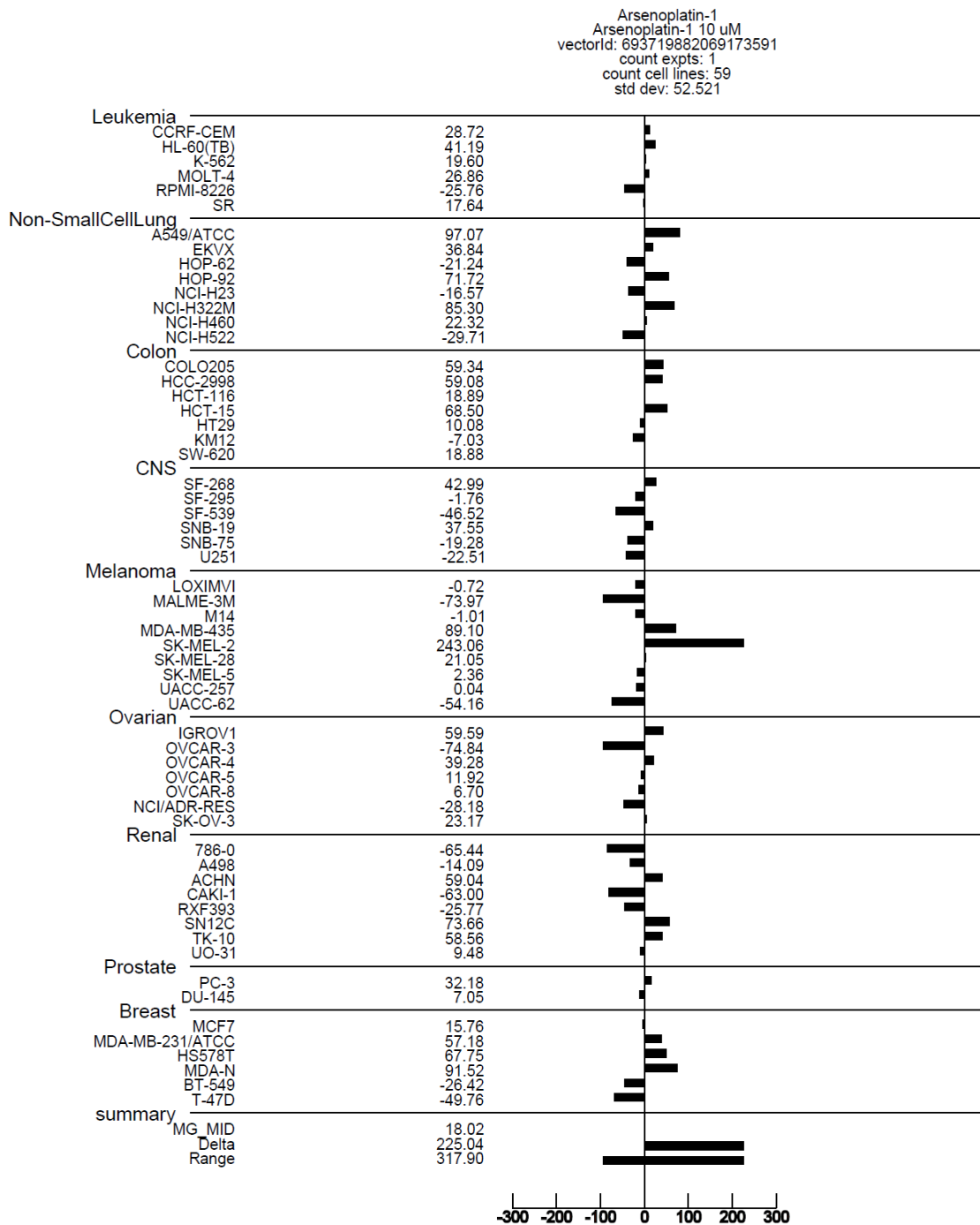


Figure S4. NCI-60 human tumor cell lines screen. One dose mean graph for Arsenoplatin-1 (AP-1).

Developmental Therapeutics Program Mean Graph
Selected Data Vectors

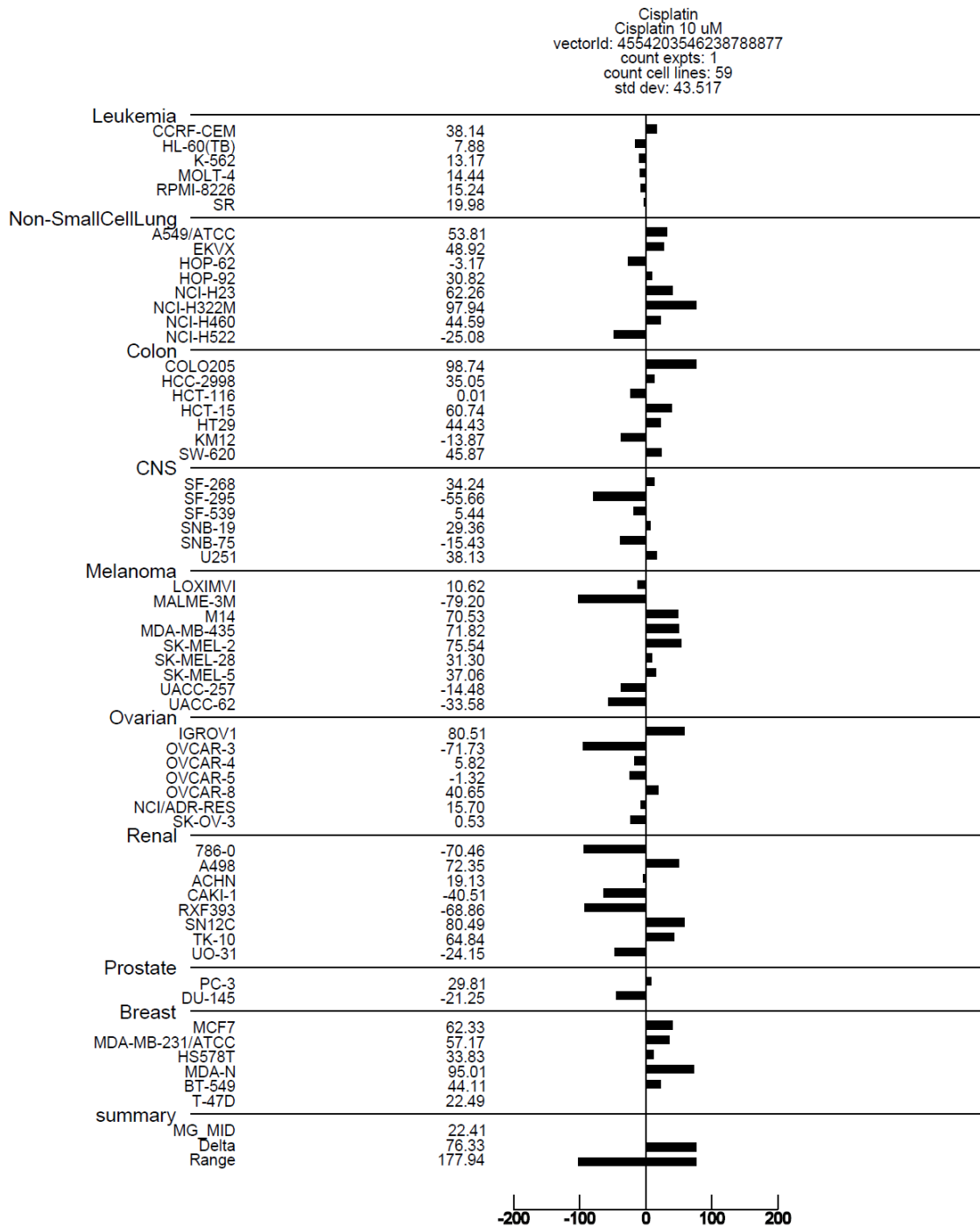


Figure S5. NCI-60 human tumor cell lines screen. One dose mean graph for Cisplatin.

Developmental Therapeutics Program Mean Graph
Selected Data Vectors

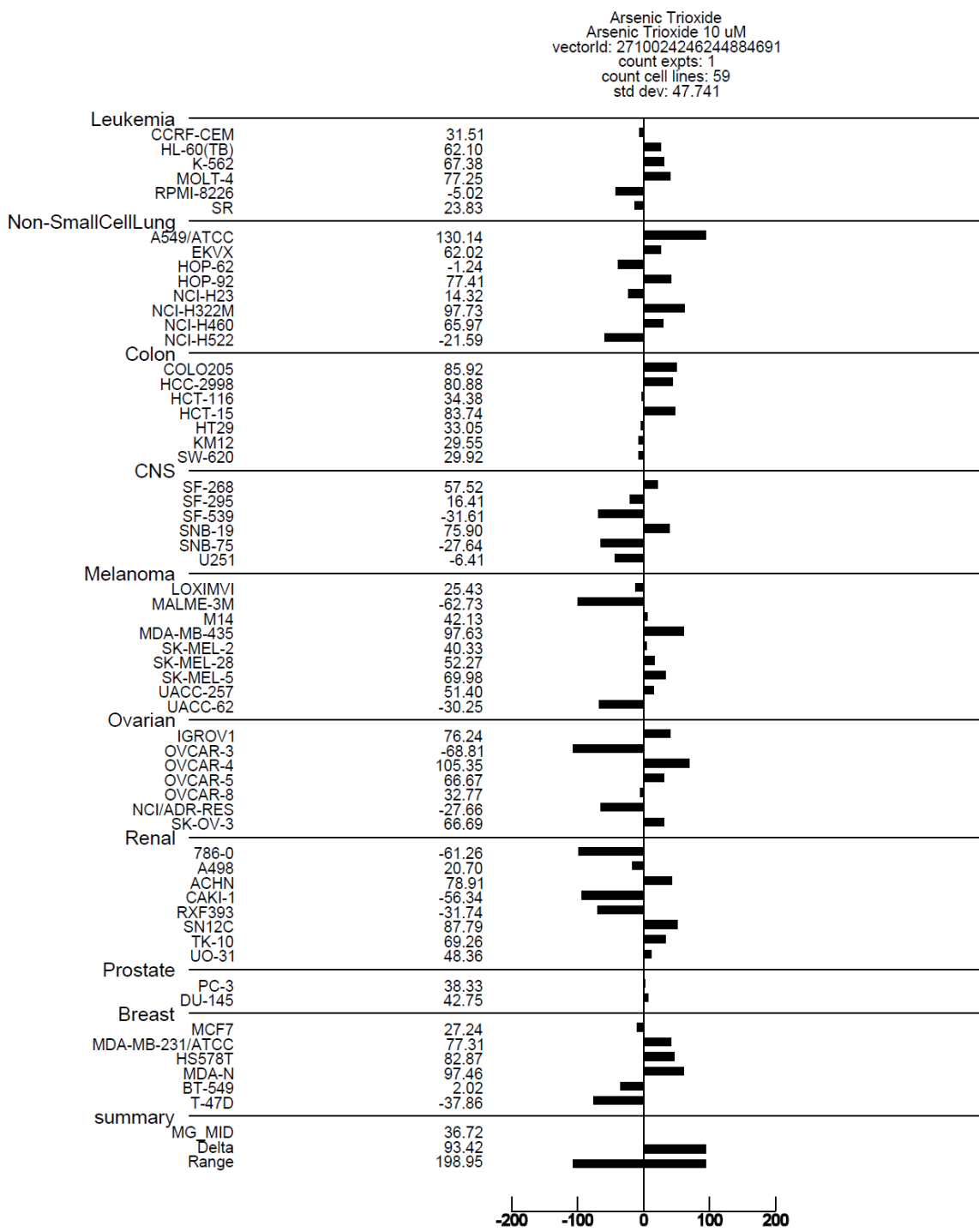


Figure S6. NCI-60 human tumor cell lines screen. One dose mean graph for Arsenic Trioxide.

NCI-60 Response and Pearson's Correlation Coefficients

Following the NCI protocol², positive values represent the growth percent, and negative values represent the % of lethality of investigated cells in the one dose-mean graphs.

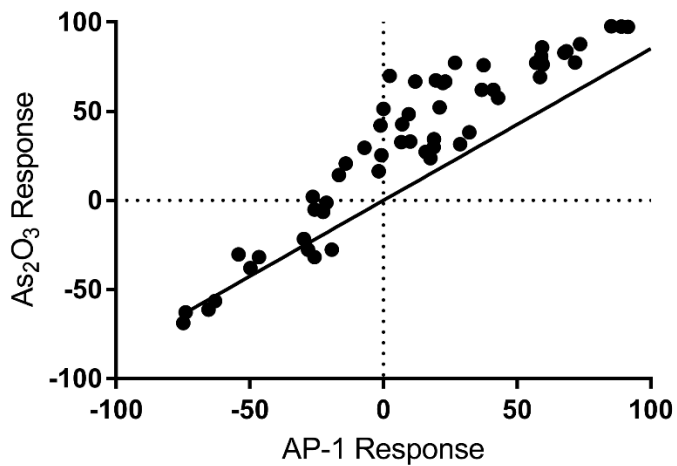


Figure S7. AP-1 vs As₂O₃ response in NCI-60. Pearson's correlation coefficient (PCC) = 0.78.

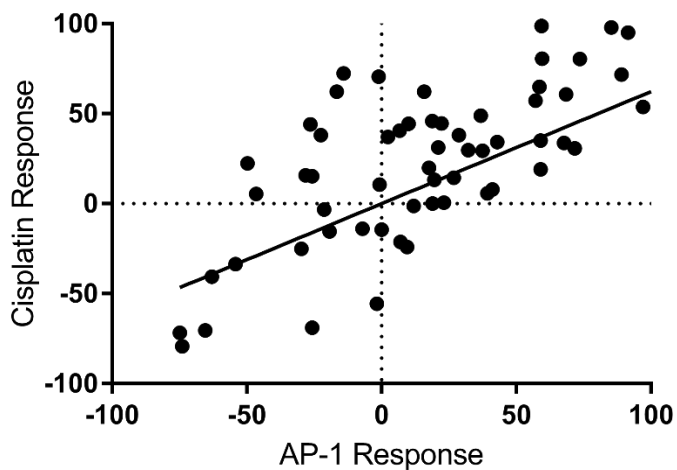
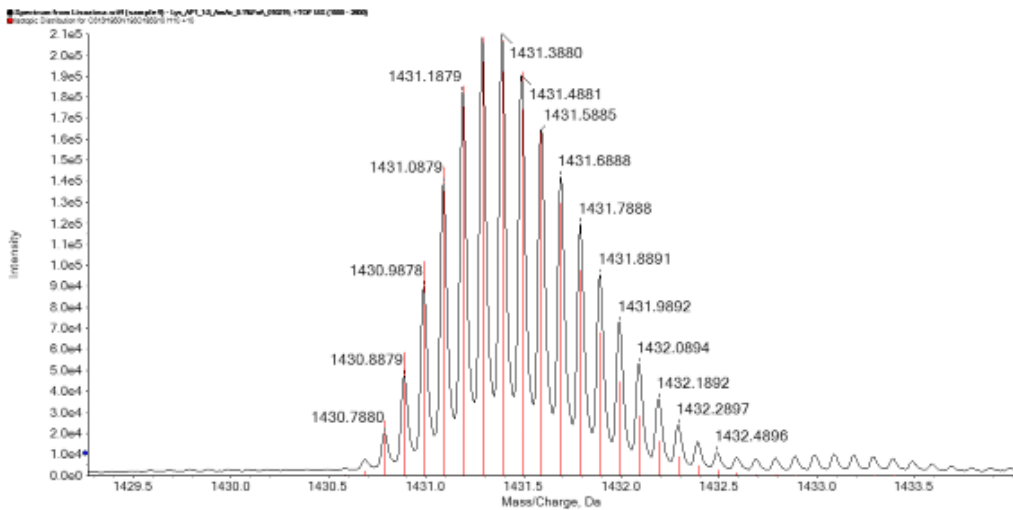


Figure S8. AP-1 vs cisplatin response in NCI-60. Pearson's correlation coefficient (PCC) = 0.67.

ESI-MS Spectra

AP-1 was reacted with lysozyme or RNase A in 20 mM ammonium acetate, pH 6.8. Metal complex to protein ratio was 3:1 with final protein concentration 10^{-4} M. Reaction mixtures were incubated for 72 h at 37 °C. Samples were diluted with LC-MS water at 10^{-6} M protein final concentration and before analysis 0.1% of FoA was also added. Respective ESI-MS spectra were acquired through direct infusion at $5 \mu\text{l min}^{-1}$ flow rate in a TripleTOF® 5600+ mass spectrometer (Sciex, Framingham, MA, U.S.A.), equipped with a DuoSpray® interface operating with an ESI probe. The ESI source parameters were optimized and were as follows: positive polarity, Ionspray Voltage Floating 5500 V, Ion source Gas 1 (GS1) 40; Curtain Gas (CUR) 25, Declustering Potential (DP) 150 V, Collision Energy (CE) 10 V. For acquisition, Analyst TF software 1.7.1 (Sciex) was used and deconvoluted spectra were obtained by using the Bio Tool Kit micro-application v.2.2 embedded in PeakView™ software v.2.2 (Sciex).



PROTEIN SEQUENCE UNIPROT>sp|P00698|LYSC_CHICK Lysozyme C OS=Gallus gallus OX=9031
GN=LYZ PE=1 SV=1
MRSLLILVLCFLPLAALGKVFGRCELAAAMKRHGLDNRYGYSLGNWVCAAKFESNFNTQA
TNRNTDGDSTDYGILQINSRWWCNDGRTPGSRNLCNIPCSALLSSDITASVNC AKKIVSDG
NGMNAWVAWRNRCKGTDVQAWIRGCR L

A)

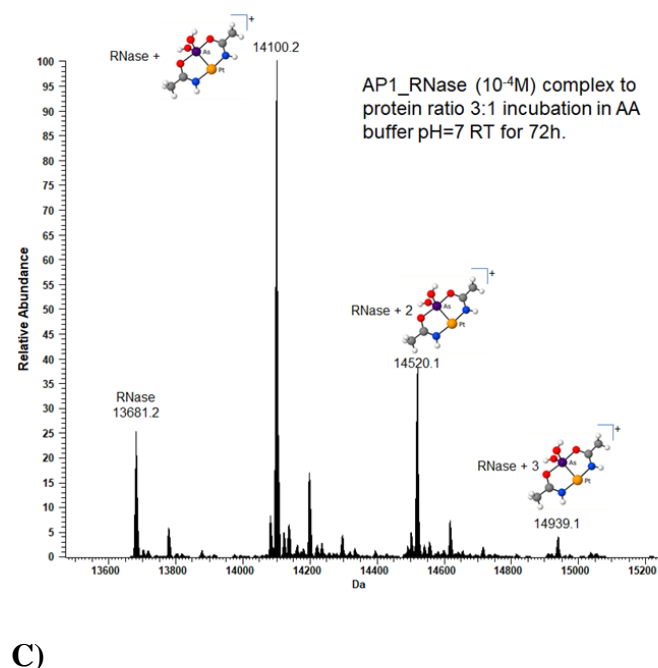
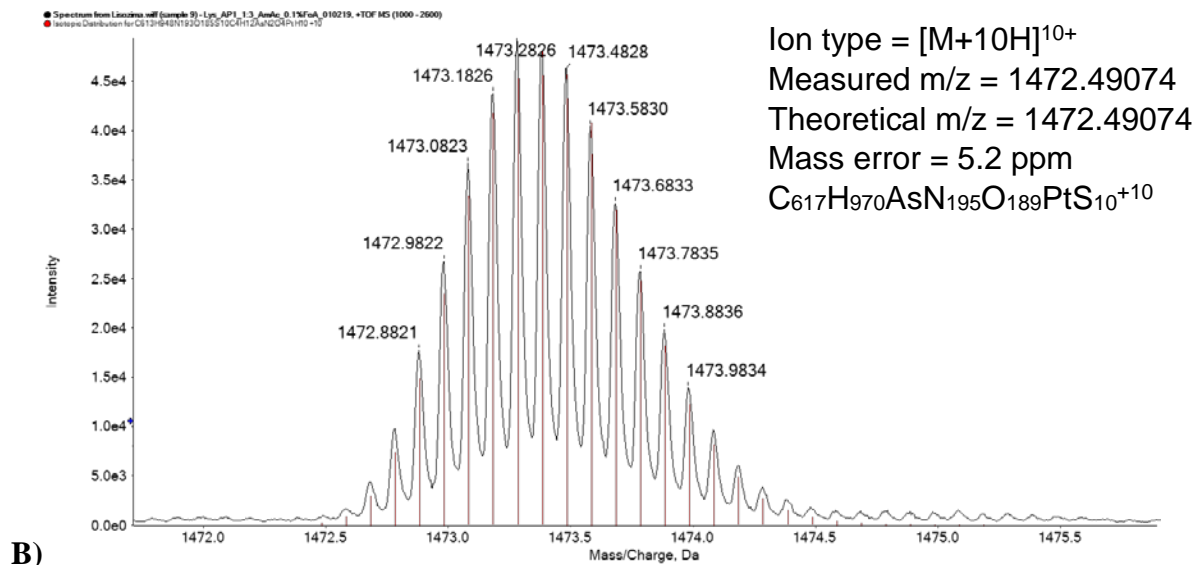


Figure S9. **A)** Theoretical simulation of lysozyme isotopic pattern (red) and experimental peak (black) (+10 charge); **B)** Theoretical simulation of AP-1-lysozyme isotopic pattern (red) and experimental peak (+10 charge) **C)** ESI MS spectrum of AP-1 ($10^{-4}M$) incubated for 72 h in 20 mM ammonium acetate buffer (pH=7) in presence of RNase A ($25^{\circ}C$). Complex to protein ratio was 3:1 (mass error calculated for the attribution < 5 ppm).

Crystallographic Data

Crystallization of AP-1 adducts with bovine pancreatic ribonuclease and hen egg white lysozyme

Bovine pancreatic ribonuclease (RNase A) and hen egg-white lysozyme (HEWL) were purchased from Sigma-Aldrich and used without further purification. RNase A was crystallized using vapor diffusion method and the hanging drop technique using protein at a concentration of 20 mg mL⁻¹ and a reservoir solution consisting of 22% w/v PEG4K, 10 mM sodium acetate pH 5.1. Crystals of RNase A-AP-1 were formed by soaking pre-grown RNase A crystals for 3 h in a solution containing 5 mM AP-1 dissolved in DMSO and then added to the reservoir. HEWL was crystallized by the vapor diffusion method, using the hanging drop technique and 1 µl of the protein at 20 mg mL⁻¹ concentration mixed with 1 µl of reservoir solution consisting of 20% ethylene glycol, 0.1 M sodium acetate at pH 4.5, 0.6 M sodium nitrate. Crystals of the HEWL adduct with AP-1 were obtained upon two days soaking of pre-grown HEWL crystals in a solution containing 5 mM AP-1 dissolved in DMSO and added to the crystal mother liquor.

Data Collection, structure solution and refinement

X-ray diffraction data from AP-1 soaked crystals of RNase A and HEWL were collected at the CNR Institute of Biostructures and Bioimages in Naples, Italy using a Cu rotating anode. In all cases, diffraction patterns were recorded at 100 K using a CCD detector with an oscillation range of 1.0 degree per frame, an exposure time of 8.0 s per frame, and a crystal-to-detector distance of 45 mm. In order to avoid possible structural heterogeneities due to the short soak in the cryo-protectant solution, datasets were collected freezing the crystals without a cryoprotectant solution, as previously done in other works.³⁻⁴ Diffraction images have been processed with the HKL2000 program suite.⁵ Statistics of the data collection are summarized in Table S2.

The structure of HEWL from PDB code 4J1A⁶ and that of RNase A from pdb code 1JVT (chain A)⁷ without water molecules and ligands were used as starting models for crystallographic refinements, which have been performed using the program REFMAC5.^{7,8} Refinement statistics are summarized in Table S3. Platinum (and thus ligand atoms) occupancies were manually adjusted, until no peaks were observed on Pt center in the difference Fourier (Fo-Fc) electron density maps. Refinements suggest Pt occupancies values in the range 0.60-0.75 with B-factors

values that fall within the range 24.3–49.2 Å². Data were deposited in the Protein Data Bank under the accession codes 5NJ1 and 5NJ7.

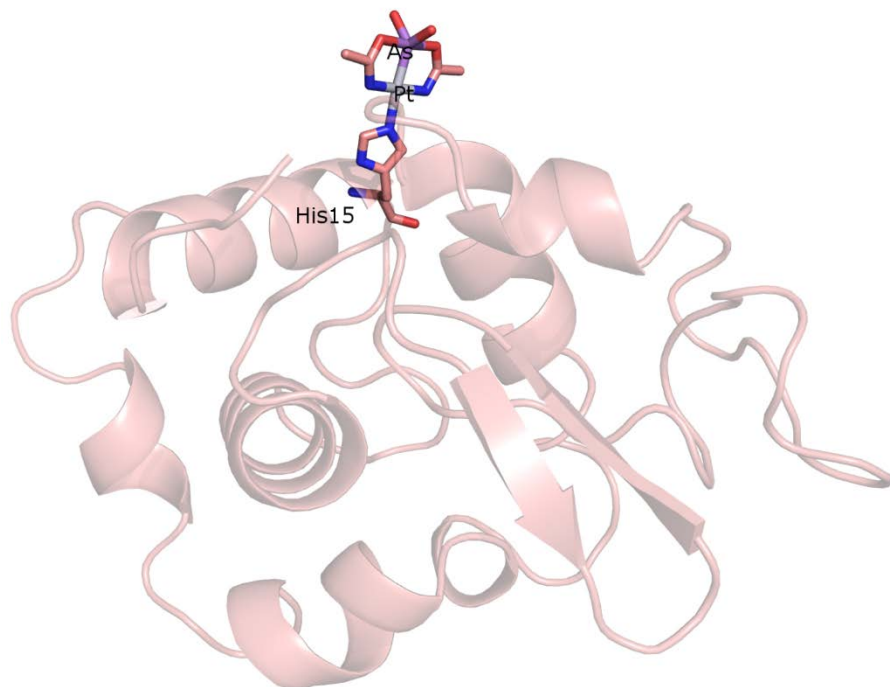


Figure S10. Arsenoplatin-1-Lysozyme adduct – ribbon representation of structure (5NJ1)

Catalytic Activity Assay

Experiments were performed using the Kunitz method⁹ at 25 °C in 0.050 M sodium acetate pH 5.0, using $0.5 \text{ mg} \times \text{mL}^{-1}$ of RNA and enzyme concentration of $0.5 \text{ } \mu\text{g} \times \text{mL}^{-1}$.

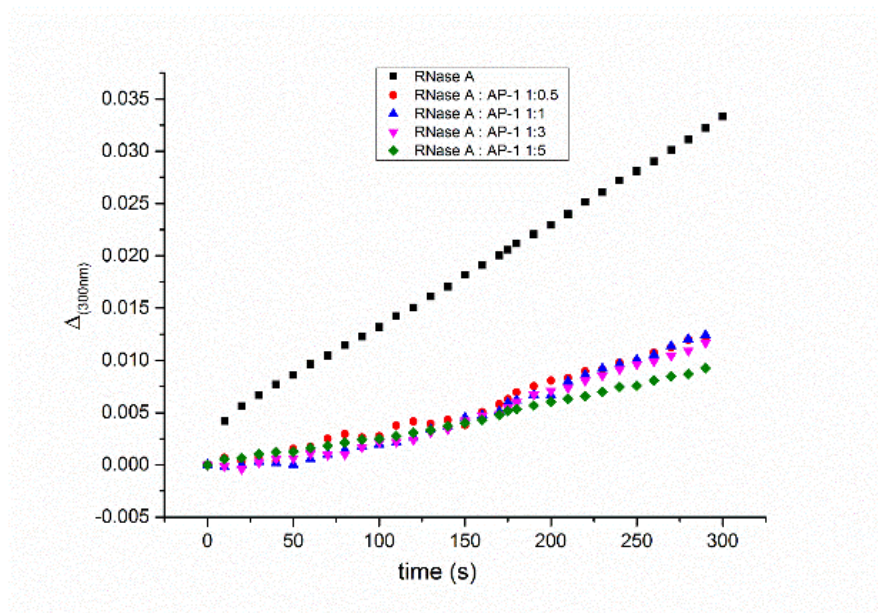


Figure S11. Hydrolysis of yeast RNA by RNase A and by RNase A-AP-1 adduct.

DNA Isolation and Determination

MDA-MB-231 (triple negative breast) cancer cells were seeded in 90 mm culture dish plates at the density of approximately 1×10^6 cells/mL at 37°C in 5% CO₂, and have grown until confluence has reached approximately 80%. Cells were exposed to final concentration of 100 μM Cisplatin and Arsenoplatin-1 for 4h and 8h. After exposure, medium with the drugs was removed and cells were washed 3x and left to grow in platinum free medium 12-20 hours (McCoy modified medium). After that period medium was removed, and cells were lysed with DNAzol Reagent (Life Technologies), 0.75-1ml DNAzol per 10 cm² culture plate area. The lysate is transferred to 10 mL tubes and centrifuged 10 min at 10,000 g at 4 °C. DNA was precipitated from the lysate by the addition of 100 % ethanol (0.5 mL of 100 % ethanol per 1 ml of DNAzol reagent). DNA was pelleted by centrifugation of sample at 4,000 x g for 5 min at 4°C and washed three times with 75% ethanol. DNA is air dried after removing the ethanol and dissolved in 8 mM NaOH. pH is adjusted to 7.5 using 0.1 M HEPES solution. The purity of the DNA was checked by measuring the absorbance of a solution at 260 and 280 nm using NanoDrop instrument. DNA-adducts were digested with 100 μL concentrated nitric acid (trace metal grade, Fisher Scientific) for measurement of arsenic (As) and platinum (Pt) concentrations by inductively coupled plasma mass spectroscopy (Thermo iCAP Q ICP-MS). The amount of platinum and arsenic in the DNA samples was expressed as pmolPt/As per μg DNA.

Dose Response Studies

Cell studies were conducted using a modified procedure based on Ahn, et al.¹⁰ Cells were plated at a concentration of 80,000 cells/mL in triplicate (50 - 100 μ L/well) onto 96 well plates, incubated overnight and then treated with drugs. After 48 hours of drug treatment while incubating at 37°C, MTS cell proliferation assay solution (10 - 20 μ L/well) was added to each well and the plates were further incubated for 3 - 4 hours at 37°C before reading the absorbance at 490 nm. Cell growth rates were expressed as a function of drug concentration on a logarithmic scale. The EC₅₀ values (the drug concentration required for 50% inhibition of cell growth) were determined by fitting to a non-linear regression sigmoidal dose-response curve using Graph Pad Prism 5 (GraphPad Software, Inc. La Jolla, CA, USA).

Synergy Calculations

EC₂₅, EC₅₀, and EC₇₅ values (the drug concentration required for 25%, 50%, and 75% inhibition of cell growth, respectively) that were calculated from sigmoidal dose response curves, as well as calculated arsenic and cisplatin only EC₂₅, EC₅₀, and EC₇₅ values, were plugged into the Chou-Talalay equation $CI = \frac{(D)_1}{(Dx)_1} + \frac{(D)_2}{(Dx)_2}$, where in the denominator, (Dx)₁ is for D₁ "alone" that inhibits a system x%, and (Dx)₂ is for D₂ "alone" that inhibits a system x%. In the numerators, (D)₁ + (D)₂ —in combination also inhibit x%. To deduce the values for (D)₁ and (D)₂ individually, we take the fact that for the combination of two drugs (D)₁ and (D)₂ at the combination ratio of (D)₁:(D)₂ = P:Q, with (D)_{1,2} = (D)₁ + (D)₂, we get (D)₁ = (D)_{1,2}* [P/(P + Q)] and (D)₂ = (D)_{1,2}* [Q/(P + Q)]. Values above 1 indicate antagonism between the drugs, values of 1 indicate additivity of the drugs, and values below 1 indicate drug synergy.¹¹

Supporting Table S1: ^{195}Pt NMR shifts

	Complex	^{195}Pt shift	$\Delta\delta$ (shift upfield upon Cl^- substitution with DMSO)
Ref. ¹	AP-1 (in $\text{DMSO-}d_6$)	-3589	
This work	AP-1 (in $\text{CH}_3\text{OH-}d_4$)	-3625	
Ref. ¹⁴	Cis-[Pt(NH ₃) ₂ Cl ₂]	-2087	
	Cis-[Pt(NH ₃) ₂ Cl(S-DMSO)] ⁺	-3145	1058
	<i>trans</i> -[Pt(NH ₃) ₂ Cl ₂]	-2086	
	<i>trans</i> -[Pt(NH ₃) ₂ (S-DMSO)Cl] ⁺	-3112	1026
Ref. ¹⁵	[Pt(en)Cl ₂]	-2345	
	[Pt(en)(S-DMSO)Cl] ⁺	-3307	962
Ref. ¹⁶	cis-[PtCl ₂ (1,4-(i-Pr) ₂ dab)]	-2300	
	cis-[PtCl(1,4-(i-Pr) ₂ -dab)(S-DMSO)] Cl	-3150	850
Ref. ¹⁷	[PtCl ₂ (H ₂ bim)]	-2319	
	[PtCl(S-DMSO)(H ₂ bim)] ⁺	-3161	842

Supporting Table S2: IC₅₀ data from synergy studies

	As:Cis = 4.5:1	As:Cis = 3:1	As:Cis =1.5:1	As:Cis = 1:1	As:Cis = 0.5:1	As:Cis = 0.25:1
IC ₅₀ for As ₂ O ₃ (As) in combination μM	8.9 \pm .6	8.1 \pm .6	6.7 \pm 0.6	5.5 \pm .6	5.2 \pm 0.5	3.4 \pm .3
IC ₅₀ for Cisplatin (Cis) in combination μM	2.0 \pm 0.1	2.7 \pm 0.2	4.4 \pm .4	5.5 \pm .6	10.4 \pm 1	13.5 \pm 1

Note two rows correspond to the IC₅₀ from the perspective of arsenic and cisplatin respectively; n=3 with each experiment consisting of 3 replications.

In the same cancer cell line, IC₅₀ value for As₂O₃ alone is 9.5 \pm 0.7 μM , for Cisplatin alone 19.3 \pm .6 μM , and for AP-1 alone is 9.5 \pm 0.3 μM ¹.

Supporting Table S3. Data collection statistics

Protein	HEWL	RNase A
Space group	P4 ₃ 2 ₁ 2	C2
Unit-cell parameters		
a, b, c (Å)	79.51, 79.51, 35.91	100.54, 32.86, 72.94
β (°)	90.00	90.17
Molecules per a. u.	1	2
Resolution (Å)	56.22-1.85 (1.88-1.85)	72.94-2.15 (2.19-2.15)
Observed reflections	58381	45145
Unique reflections	10091	13274
Completeness (%)	97.7 (87.6)	99.7 (100)
Rmerge [†]	0.084 (0.487)	0.117 (0.504)
I/ σ (I)	24.9 (2.0)	10.0 (2.9)
Multiplicity	5.8 (3.4)	3.4 (3.2)

Supporting Table S4. Refinement statistics

PDB code	5NJ1	5NJ7
Protein	HEWL	RNase A
Space group	P4 ₃ 2 ₁ 2	C2
<i>Unit-cell parameters a, b, c (Å),</i> <i>β (°)</i>	79.51, 79.51, 35.91 90.00	100.54, 32.86, 72.94 90.17
Molecules per asymmetric unit	1	2
Resolution	56.22-1.85	72.94-2.15
Number of reflections used in the working set/test set	9573/491	12526/681
R factor/Rfree (%)	18.2/24.2	18.7/25.0
Non-H atoms used in the refinement	1181	2116
Number of Pt atoms in the structure	1	4 (2 Pt atoms in each RNase A chain)
Number of As atoms in the structure	1	4 (2 As atoms in each RNase A chain)
Average B-factor	35.6	33.7
Occupancy of Pt atoms	0.60	0.60/0.60/0.75/0.70
Occupancy of As atoms	0.60	0.60/0.60/0.75/0.70
B-factor of Pt atoms	24.3	40.8/41.1/43.3/49.2
B-factor of As atoms	25.6	54.4/54.7/58.1/66.6
<i>Ramachandran values</i>		
Most favored /Allowed (%)	97.4/2.6	93.6/5.1
Generously allowed/disallowed (%)	0	1.3

Lipinski Rule of Five and log*P* determination

Measurement of log *P*

Log *P* values are determined by the standard shake-flask method. Briefly, weighted amounts of AP-1 and AP-2 were partitioned between equal volumes of MQ water and n-octanol for 3h at room temperature (25 °C). The concentration of platinum in the aqueous and octanol phase was determined by ICP-MS. The log *P*_{o/w} values are calculated as the logarithm of the concentration ratio of the substance in two-phase system using the following equation¹⁸:

$$\text{Log } P_{o/w} = \log \frac{C_o - C_w}{C_w}$$

Supporting Table S5. Lipinski rule of five and log*P* values

	log <i>P</i>	Ref.	Molecular weight (g/mol)	H-bond donors	H-bond acceptors
Cisplatin	-2.30 average (-2.19, -2.53, -2.28, -2.27)	¹⁹⁻²⁰	300.01	2	2
Oxaliplatin	-1.54 average (-1.65, -1.64, -1.39)	¹⁹⁻²⁰	429.29	4	8
Carboplatin	-1.64 average (-2.30, -1.39, -1.63)	¹⁹⁻²⁰	373.06	4	6
Satraplatin (in clinical trials)	-0.16	¹⁹	502.30	4	6
Arsenoplatin-1	-0.99	This work	455.56	4	6
Arsenoplatin-2 ¹	-0.18	This work	483.62	4	6

According to the Lipinski's Rule of Five – a compound will have sufficient absorption after oral dosing if contains: not more than 5 hydrogen bond donors (nitrogen or oxygen atoms with one or more hydrogen atoms); not more than 10 hydrogen bond acceptors (nitrogen or oxygen atoms), a molecular weight under 500, and a partition coefficient log *P* less than 5²¹⁻²².

References:

1. Miodragović, Đ. U.; Quentzel, J. A.; Kurutz, J. W.; Stern, C. L.; Ahn, R. W.; Kandela, I.; Mazar, A.; O'Halloran, T. V., Robust Structure and Reactivity of Aqueous Arsenous Acid–Platinum(II) Anticancer Complexes. *Angewandte Chemie International Edition* **2013**, *52* (41), 10749-10752.
2. Holbeck, S. L.; Collins, J. M.; Doroshow, J. H., Analysis of Food and Drug Administration–Approved Anticancer Agents in the NCI60 Panel of Human Tumor Cell Lines. *Molecular Cancer Therapeutics* **2010**, *9* (5), 1451-1460.
3. Russo Krauss, I.; Messori, L.; Cinellu, M. A.; Marasco, D.; Sirignano, R.; Merlino, A., Interactions of gold-based drugs with proteins: the structure and stability of the adduct formed in the reaction between lysozyme and the cytotoxic gold(III) compound Auoxo3. *Dalton Transactions* **2014**, *43* (46), 17483-17488.
4. Messori, L.; Cinellu, M. A.; Merlino, A., Protein Recognition of Gold-Based Drugs: 3D Structure of the Complex Formed When Lysozyme Reacts with Aubipyc. *ACS Medicinal Chemistry Letters* **2014**, *5* (10), 1110-1113.
5. Otwinowski, Z.; Minor, W., [20] Processing of X-ray diffraction data collected in oscillation mode. *Methods in Enzymology* **1997**, *276*, 307-326.
6. Vergara, A.; D'Errico, G.; Montesarchio, D.; Mangiapia, G.; Paduano, L.; Merlino, A., Interaction of Anticancer Ruthenium Compounds with Proteins: High-Resolution X-ray Structures and Raman Microscopy Studies of the Adduct between Hen Egg White Lysozyme and AziRu. *Inorganic Chemistry* **2013**, *52* (8), 4157-4159.
7. Vitagliano, L.; Merlino, A.; Zagari, A.; Mazzarella, L., Reversible substrate-induced domain motions in ribonuclease A. *Proteins: Structure, Function, and Bioinformatics* **2002**, *46* (1), 97-104.
8. Murshudov, G. N.; Skubak, P.; Lebedev, A. A.; Pannu, N. S.; Steiner, R. A.; Nicholls, R. A.; Winn, M. D.; Long, F.; Vagin, A. A., REFMAC5 for the refinement of macromolecular crystal structures. *Acta Crystallographica Section D* **2011**, *67* (4), 355-367.
9. Kunitz, M., A SPECTROPHOTOMETRIC METHOD FOR THE MEASUREMENT OF RIBONUCLEASE ACTIVITY. *Journal of Biological Chemistry* **1946**, *164* (2), 563-568.
10. Ahn, C.; Ahn, D., Randomized Clinical Trials in Stroke Research. *Journal of investigative medicine : the official publication of the American Federation for Clinical Research* **2010**, *58* (2), 277-281.
11. Chou, T.-C., Drug Combination Studies and Their Synergy Quantification Using the Chou-Talalay Method. *Cancer Research* **2010**, *70* (2), 440-446.
12. Bednarek, E.; Sitkowski, J.; Kawęcki, R.; Kozerski, L.; Bocian, W.; Pazderski, L.; Priebe, W., Structure and dynamics of methylcis-3,4-diamino-2,3,4,6-tetra-deoxy- α -l-lyxo-hexopyranoside complexes with PtCl₂ and PdCl₂, by ¹H, ²H, ¹³C, ¹⁵N and ¹⁹⁵Pt NMR spectroscopy in DMSO, CD₃CN and H₂O. *Dalton Transactions* **2008**, (31), 4129-4137.
13. Dodoff Nicolay, I.; Kovala-Demertzi, D.; Kubiak, M.; Kuduk-Jaworska, J.; Kochel, A.; Gorneva Galina, A., Dimethyl Sulfoxide Containing Platinum(II) and Palladium(II) Chelate Complexes of Glyoxylic and Pyruvic Acid Thiosemicarbazones. A New Class of Cytotoxic Metal Complexes. In *Zeitschrift für Naturforschung B*, 2006; Vol. 61, p 1110.
14. Sundquist, W. I.; Ahmed, K. J.; Hollis, L. S.; Lippard, S. J., Solvolysis reactions of cis- and trans-diamminedichloroplatinum(II) in dimethyl sulfoxide. Structural characterization and DNA binding of trans-bis(ammine)chloro(DMSO)platinum(1+). *Inorganic Chemistry* **1987**, *26* (10), 1524-1528.
15. Kerrison, S. J. S.; Sadler, P. J., ¹⁹⁵Pt NMR studies of platinum(II) dimethylsulphoxide complexes. *Inorganica Chimica Acta* **1985**, *104* (3), 197-201.
16. Fanizzi, F. P.; Intini, F. P.; Maresca, L.; Natile, G.; Uccello-Barretta, G., Solvolysis of platinum complexes with substituted ethylenediamines in dimethyl sulfoxide. *Inorganic Chemistry* **1990**, *29* (1), 29-33.

17. Casas, J. S.; Castiñeiras, A.; Parajó, Y.; Pérez-Parallé, M. L.; Sánchez, A.; Sánchez-González, A.; Sordo, J., Pd(II) and Pt(II) complexes of 2,2'-biimidazole and its N,N'-dimethyl derivative. The crystal structure of [PtBr(DMSO)}₂(Me₂bim)] (Me₂bim=N,N'-dimethyl-2,2'-biimidazole). *Polyhedron* **2003**, *22* (8), 1113-1121.
18. Foteeva, L. S.; Trofimov, D. A.; Kuznetsova, O. V.; Kowol, C. R.; Arion, V. B.; Keppler, B. K.; Timerbaev, A. R., A quantitative structure–activity approach for lipophilicity estimation of antitumor complexes of different metals using microemulsion electrokinetic chromatography. *Journal of Pharmaceutical and Biomedical Analysis* **2011**, *55* (3), 409-413.
19. Oldfield, S. P.; Hall, M. D.; Platts, J. A., Calculation of Lipophilicity of a Large, Diverse Dataset of Anticancer Platinum Complexes and the Relation to Cellular Uptake. *Journal of Medicinal Chemistry* **2007**, *50* (21), 5227-5237.
20. Screnci, D.; McKeage, M. J.; Galettis, P.; Hambley, T. W.; Palmer, B. D.; Baguley, B. C., Relationships between hydrophobicity, reactivity, accumulation and peripheral nerve toxicity of a series of platinum drugs. *Br J Cancer* **2000**, *82* (4), 966-972.
21. Leeson, P., Drug discovery: Chemical beauty contest. *Nature* **2012**, *481* (7382), 455-456.
22. Kerns, E. H.; Di, L., Chapter 5 - Lipophilicity. In *Drug-like Properties: Concepts, Structure Design and Methods*, Academic Press: San Diego, 2008; pp 43-47.